The Role of Stoichiometry on Ordering Phase Transformations in Ni–Cr Alloys for Nuclear Applications

Fei Teng, Li-Jen Yu, Octav Ciuca, Emmanuelle Marquis, Grace Burke and Julie D. Tucker

Abstract Mechanical property degradation due to isothermal ageing is of potential concern for alloys based on the Ni–Cr binary system, such as Alloys 625 and 690. The disorder-order phase transformation, which is the primary source of embrittlement, has been studied in Ni–Cr model alloys by experimental approaches. Model alloys with different stoichiometries have been isothermally aged up to 5000 h at three temperatures (373, 418, and 475 °C) and characterized via nano-indentation, atom probe tomography, and transmission electron microscopy. Results show that off-stoichiometry alloys exhibit ordering but at a slower rate than stoichiometric (Ni/Cr = 2.0) alloy.

Keywords Stoichiometry · Ordering · Ni-based · Model alloys

F. Teng (✉) · J.D. Tucker
Oregon State University, Corvallis, OR 97331, USA
e-mail: tengf@oregonstate.edu

J.D. Tucker
e-mail: Julie.Tucker@oregonstate.edu

L.-J. Yu · E. Marquis
University of Michigan, Ann Arbor, MI 48109, USA
e-mail: ljezrayu@umich.edu

E. Marquis
e-mail: emarq@umich.edu

O. Ciuca · G. Burke
University of Manchester, Manchester M13 9PL, UK
e-mail: Octav.Ciuca@manchester.ac.uk

G. Burke
e-mail: M.G.Burke@manchester.ac.uk

J.H. Jackson et al. (eds.), *Proceedings of the 18th International Conference on Environmental Degradation of Materials in Nuclear Power Systems – Water Reactors*, The Minerals, Metals & Materials Series, https://doi.org/10.1007/978-3-030-04639-2_16

Introduction

The primary life-limiting factor for light water reactors (LWR) is the environmental degradation of reactor components due to radiation damage, corrosion, and high temperature phase transformation. Key components, such as reactor pressure vessel heads and steam generators, are difficult and costly to replace, which makes lifetime extension an important factor in reactor plant license renewal and safety evaluation. Ni-based alloys are widely used in nuclear plants due to their excellent corrosion resistance, fracture toughness, and phase stability during ageing.

Primary components that are now being made with Ni-based (e.g. Alloys 690 and 625) alloys include: steam generator tubing, reactor pressure vessel heads, and control rod drive mechanism penetrations, which are designed for relatively high temperatures ($\sim$300 °C) and necessary long lifetimes. The Ni/Cr ratio of these commercial alloys is possibly located in the ordering phase transformation field of the Ni–Cr phase diagram (from 0.65 to 0.7 Ni%) [1]. There is little experimental data in this region to confirm the extent of the ordered phase. Ordering occurs when the attractive force between different atoms is larger than that of same atoms. Thus during the ordering transformation of Ni–Cr system, atoms rearrange from random solid solution into regular patterns [2] (layers of Ni and Cr in $MoPt_2$-type structure shown in Fig. 1) below a critical temperature, T_c = 590 °C [1]. If the alloy is in the ordered phase region or in a two-phase region (bcc Cr + $MoPt_2$), the ordered phase will nucleate and grow [3–7]. Based on the result from previous research on binary Ni–Cr alloys, the ordered phase can cause an increase in tensile strength, a decrease in ductility, and dimensional changes or internal stresses. Previous research results also show a hardening effect from ordering and a linear relationship between Vickers microhardness and yield strength [8]. It is known that the fracture toughness decreases as yield strength increases, and fracture toughness is a key factor in stress corrosion crack (SCC).

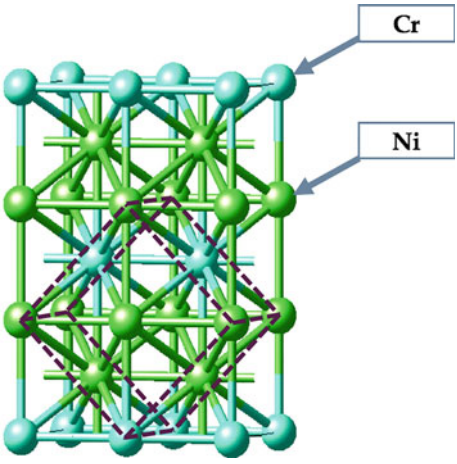

Fig. 1 Sketch of $MoPt_2$ structure (solid line) with a FCC cell (broken line)

The main objectives of this project are to define the relationship between the disorder-order transformation and stoichiometries in the phase diagram. To accomplish the goals, four Ni–Cr binary model alloys with different stoichiometries were isothermally aged and characterized to determine the range of thermal embrittlement susceptibility.

Experimental Methods

The binary model alloys were made in stoichiometry ratios of Ni/Cr (at.%) of 1.8, 2.0, 2.2, and 2.4 to explore the unknown region of the phase diagram of Ni–Cr under 500 °C. Samples were fabricated by small batch (~300 g) arc-melting, then hot-rolled, homogenized in a furnace for 24 h at 1093 °C and water-quenched to room temperature. Compositional analysis was performed by a third-party test laboratory based on method CAP-017 N (ICP-AES) and ASTM 1019-11 (Comb./IGF) (Table 1).

Alloy button plates were cut into 10 × 10 × 5 mm^3 specimens by electrical discharge machining to minimize heat generation during the cutting process. All alloys (four stoichiometries) were heat-treated at three temperatures. 373, 418, and 475 °C, for up to 10,000 h. The heat treatment test matrix is shown in Table 2.

For micro-hardness tests, the surfaces of samples were ground using SiC papers from 240 to 800 grit followed by 0.05 μm colloidal SiO_2 polishing. Micro-hardness measurements were performed using a Micromaterials Vantage nanoindenter with a Berkovich diamond tip and a load of 500 mN. The load was chosen to balance degradation of indenter tip, sensitivity for vibration from environment during testing, resistance on effect of grain orientation, effect of grain boundary on indentation, and the accuracy level of result. A larger load causes faster tip damage, which changes the dynamic area function that used to calculate micro-hardness. A smaller load requires lower environmental vibration. Additionally, grain orientation and presence of grain boundaries will have a greater effect for a low indentation load than for a high load when measuring mirco-hardness. Considering these requirements, microhardness measurements using a grid of (4 × 5) were performed on the sample surface with an distance of 600 μm between indentations.

Table 1 Composition of binary model Ni–Cr alloys (at.%)

Element	Ratio 1.8	Ratio 2.0	Ratio 2.2	Ratio 2.4
C	0.05	0.05	0.05	0.05
Cr	35.66	33.24	31.10	29.83
Fe	<0.01	<0.01	<0.01	<0.01
P	<0.01	<0.01	<0.01	<0.01
S	<0.002	<0.002	<0.002	<0.001
Ni	64.27	66.69	68.83	70.10
Ni/Cr	1.80	2.01	2.21	2.35

Table 2 Heat treatment test matrix of binary model Ni–Cr alloys

Temperature (°C)	Time (h)				
	500	1000	3000	5000	10,000
373	4	4	4	4	4
418	4	4	4	4	4
475	4	4	4	4	4

Transmission electron microscopy (TEM) specimens were prepared by jet electro-polishing in 20% $HClO_{4–8}$0% CH_3OH at −35 °C using a Struers Tenupol 5 with a Julabo FP50 closed-cycle refrigeration system. Microstructural characterization of the aged Ni–Cr samples was performed using the FEI Tecnai F30 and FEI Talos F200 field emission gun analytical transmission electron microscopes.

Atom probe tomography (APT) specimens were prepared using an FEI Nova 200 Nanolab FIB. APT specimens were fabricated by utilizing concentric annular milling with a series of decreasing ion currents at 30 kV applied voltage and a 5 kV final milling step. Data were collected using a Cameca LEAP 4000× HR operated in voltage mode using a 20% pulse fraction, 200 kHz pulse rate, and a target detection rate of 0.5% at 50 K. Reconstructions were performed using the IVAS 3.6.12 software. Reconstruction parameters were adjusted to ensure uniform axial and radial density, which resulted in image compression factor values in the range of 1.2–1.7 and k-factor values between 3.3 and 3.5. The evaporation field was taken as that of Ni, 35 V/nm.

Results and Discussion

Transmission Electron Microscopy

The Ni–Cr alloys were characterized by a fully recrystallized equiaxed grain structure; the grain size ranged from 70 to 360 µm. Selected area electron diffraction (SAED) was used to assess the formation of the ordered Pt_2Mo-type Ni_2Cr precipitates during ageing. The strategy to characterize Pt_2Mo-type ordered structure in Ni–Cr alloys via TEM has been well documented in previous research [3, 5, 8, 9]. The additional reflections in the electron diffraction patterns were analyzed to confirm the formation of Ni_2Cr precipitates. Figure 2 shows the evolution of secondary reflection in Ni/Cr = 2.0 sample. Note that no Ni_2Cr precipitate reflections were detected in the specimens aged at 373 °C or 418 °C for 3000 h, but the presence of Ni_2Cr was confirmed after 3000 h at 475 °C.

The nano-scale Ni_2Cr precipitates formed during ageing at 475 °C are shown in the dark-field TEM image in Fig. 3a. These ultra-fine intragranular Ni_2Cr precipitates were less than 5 nm in size. The TEM observations are summarized in Table 3.

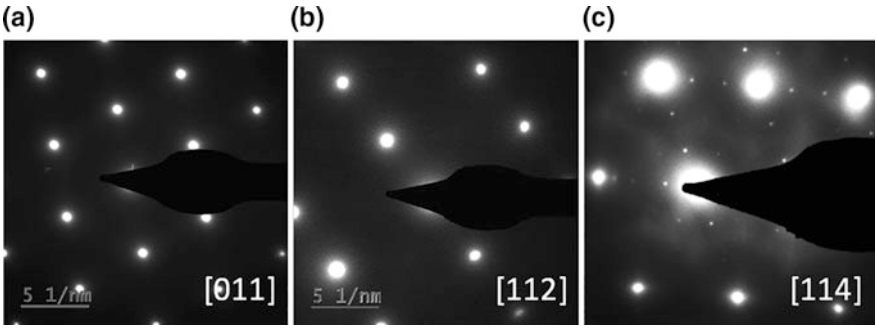

Fig. 2 TEM SAED patterns obtained from Ni/Cr = 2.0 specimens aged for 3000 h at: **a** 373 °C ([011] zone axis); **b** 418 °C ([112] zone axis); and **c** 475 °C ([114] zone axis, ordered precipitate reflection can be observed at 1/3 and 2/3 $\{311\}_{matrix}$ and $\{220\}_{matrix}$)

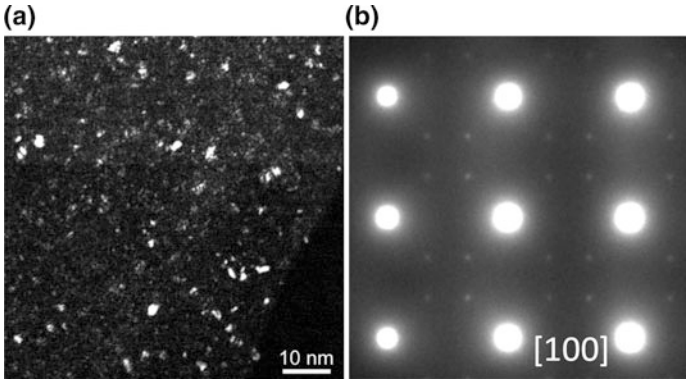

Fig. 3 **a** Dark-field TEM image of the Ni_2Cr precipitates, and **b** corresponding [100] SAED pattern showing the ordered precipitate reflections at equivalent 1/3 and 2/3 $\{220\}_{matrix}$ for Ni/Cr = 2.0 aged at 475 °C for 5000 h

Table 3 TEM characterization results for Ni/Cr = 2.0 samples

Sample	Intragranular precipitates	Secondary reflection
2.0–373 °C–3000 h	No	No
2.0–418 °C–3000 h	No	No
2.0–475 °C–3000 h	<5 nm	Yes
2.0–475 °C–5000 h	<5 nm	Yes

Atom Probe Tomography

Atom probe tomography was used to identify the extent of the ordering transformation. The characterization of Pt_2Mo-type precipitates is challenging because of similar matrix and precipitate compositions and evaporation artifacts that lead to significant density variations in the reconstructed data that remain to be explained. These density variations are visible in Fig. 4 (left). Nonetheless, the ordered phase can still be detected by APT using appropriately oriented specimens so that the ordered lattice planes are visible in the datasets [10, 11]. Such an ordered precipitate is highlighted in Fig. 4. The composition of the ordered precipitates was measured from several cube regions encompassing the ordered precipitates, as the one in Fig. 4 but smaller to ensure that the region does not exceed the precipitate. The measured precipitate composition shown in Table 4 agrees with the expected stoichiometry.

Micro-hardness

The micro-hardness of model alloys as a function of ageing time at three temperatures, 373, 418, and 475 °C, is shown in Fig. 5. At 475 °C (Fig. 5a), the stoichiometric samples have a higher ordering rate than off-stoichiometric samples. For off-stoichiometric samples, the behavior is similar to the low temperature exposure, which means stoichiometric samples experience a faster ordering rate than off-stoichiometric samples. Additionally, behaviors of micro-hardness start getting stable after 1000 h, which indicates ordering transformation is approaching equilibrium. Considering the change of micro-hardness comes from ordering phase, lower amount of ordered phase has been formed in off-stoichiometric samples than in-stoichiometric samples. Based on the relationship between micro-harness and ageing time, comparison of ordered phase fraction between all samples is $2.0 > 1.8 \approx 2.2 > 2.4$.

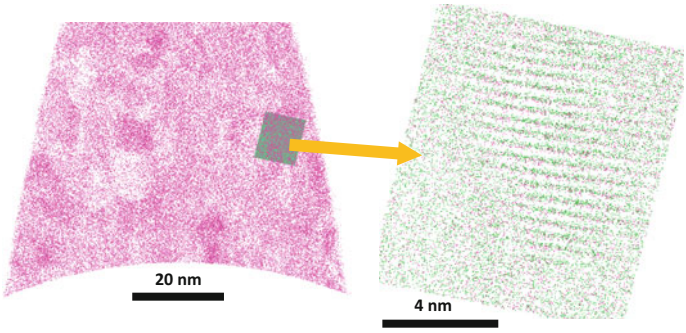

Fig. 4 Slices from APT datasets showing Cr atoms in pink (left) and Ni (green) and Cr atoms in the ordered precipitates (right). The thickness of the left slice is 2 nm, and that of the right is 5.5 nm

Table 4 The composition of Ni_2Cr precipitates after ageing at 475 °C for 10,000 h

Element	Ni	Cr
Ni/Cr 2.0	63.3–68.6%	31.3–36.6%

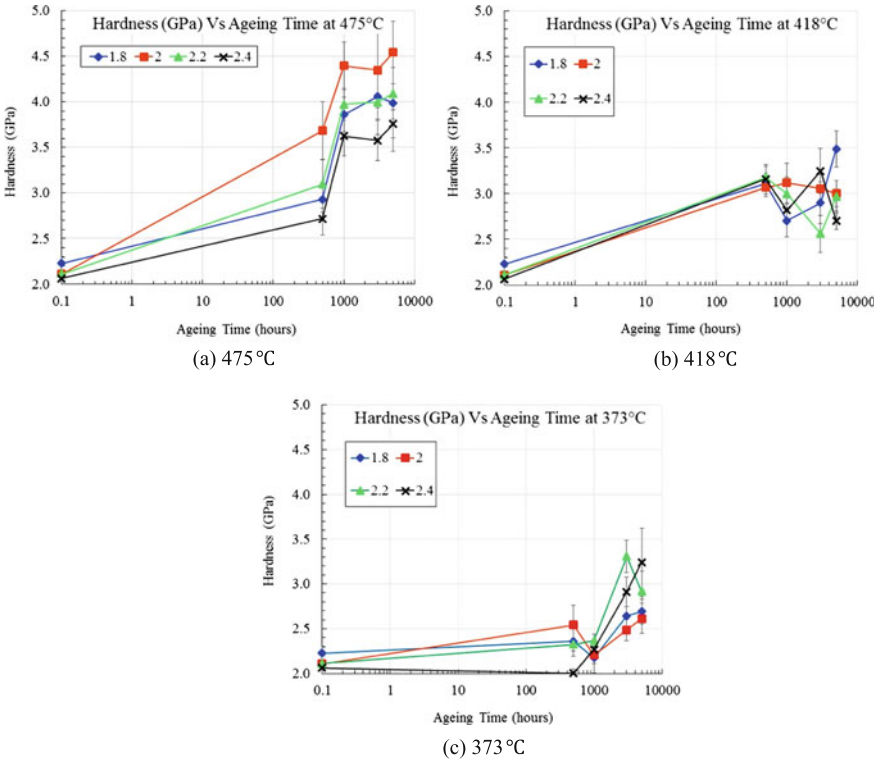

(a) 475 °C (b) 418 °C

(c) 373 °C

Fig. 5 Micro-hardness versus Ageing time at 373, 418, and 475 °C. °C for Ni/Cr ratios or 1.8, 2, 2.2 and 2.4

At 418 °C (Fig. 5b), the ordering behavior is similar for all compositions. Different degrees of hardening can be observed at all compositions. Due to the higher ageing temperature and higher diffusivity of chromium at this temperatures, the rate of hardening (or ordering) is faster than that at 373 °C. The microhardness results for the samples aged at 373 °C are presented in Fig. 5c, which shows a unclear relationship between micro-hardness and ageing time for both stoichiometric samples (Ni/Cr = 2.0) and off-stoichiometric samples due to the small change on micro-hardness and large uncertainty. All samples show a similar tendency of embrittlement.

The trend of change in micro-hardness (Fig. 5) shows that the effect of hardening will reach saturation after 1000 h of heat treatment at 475 °C, whereas the

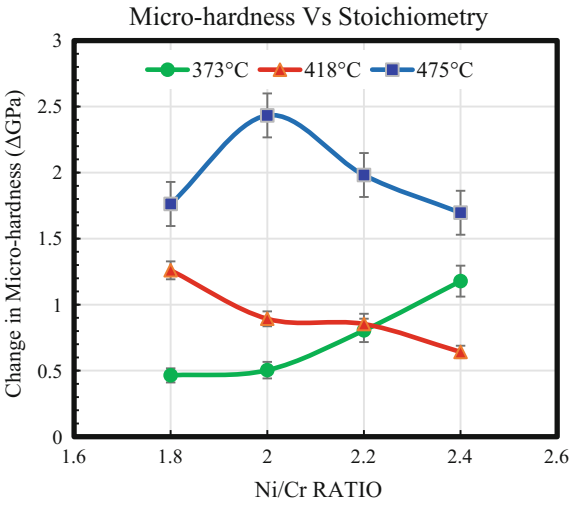

Fig. 6 Change in micro-hardness as a function of Ni/Cr stoichiometry after 5000 h ageing treatment at 373, 418, and 475 °C

time to saturation for 418 and 373 °C will be longer. By comparing the change in micro-hardness after ageing for 5000 h, which is shown in Fig. 6, the relationship between embrittlement and stoichiometry can be observed. The larger deviation from stoichiometry leads to less embrittlement.

Conclusions

In this paper, the role of stoichiometry on the Ni–Cr ordering transformation was studied by micro-hardness and the extent of precipitation was confirmed by TEM (imaging and SAED) and APT. The study shows that the Ni_2Cr precipitates have an obvious hardening effect on the Ni–Cr alloys. Fine intragranular precipitates (<5 nm) were observed via TEM after disorder-order transformation. The superlattice structure caused by increased local atomic density was detected by APT, whereas the difference in composition between precipitates and matrix phase is insignificant and cannot be used to distinguish them.

The micro-hardness data shows that stoichiometry alloys (Ni/Cr = 2.0) order more rapidly than off-stoichiometry alloys. Larger deviations from stoichiometry leads to slower ordering rates. Off-stoichiometry Ni–Cr samples are not immune to disorder-order transformation, which suggests that off-stoichiometry commercial alloys may exhibit a hardening effect from the Pt_2Mo-type ordered phase. In the model alloys, hardening due to Ni_2Cr achieved equilibrium after 1000 h ageing at 475 °C. The saturation limit for intermediate (418 °C) and low (373 °C) temperatures is still unclear because of sluggish kinetics.

Acknowledgements The authors would like to acknowledge funding from the Nuclear Energy University Program (NEUP) of DOE. This material is based upon work supported by the National Science Foundation via the Major Research Instrumentation (MRI) Program under Grant No. 1040588. We also acknowledge the Murdock Charitable Trust and the Oregon Nanoscience and Microtechnologies Institute (ONAMI) for their financial contributions towards the OSU Titan TEM. The authors (Burke and Ciuca) gratefully acknowledge funding from Program EP/N017854/1 from the UK Engineering and Physical Sciences Research Council. The author (Emmanuelle and Li-Jen) would also like to acknowledge technical support from the Michigan Center for Materials Characterization.

References

1. W. Xiong, in *Thermodynamic and Kinetic Investigation of the Fe–Cr–Ni System Driven by Engineering Applications*. Department of Materials Science and Engineering (KTH Royal Institute of Technology: School of Industrial Engineering and Management, 2012)
2. L. Guttman, in *Order-Disorder Phenomena in Metals*, ed. by S. Frederick, T. David. Solid State Physics (Academic Press, 1956), pp. 145–223
3. A. Marucco, B. Nath, Effects of ordering on the properties of Ni–Cr alloys. J. Mater. Sci. **23** (6), 2107–2114 (1988)
4. A. Marucco, Atomic ordering and α′-Cr phase precipitation in long-term aged Ni_3Cr and Ni_2Cr alloys. J. Mater. Sci. **30**(16), 4188–4194 (1995)
5. A. Marucco, Atomic ordering in the Ni Cr Fe system. Mater. Sci. Eng., A **189**(1), 267–276 (1994)
6. A. Marucco, Effects of composition on the order-disorder transformation in Ni–Cr based alloys, in *Key Engineering Materials* (Trans. Tech. Publ., 1991)
7. A. Marucco, Phase transformations during long-term ageing of Ni Fe Cr alloys in the temperature range 450–600 °C. Mater. Sci. Eng., A **194**(2), 225–233 (1995)
8. G. Young, D. Eno, Long range ordering in model Ni–Cr–X alloys, in *Fontevraud 8—Contribution of Materials Investigations and Operating Experience to LWRs' Safety, Performance and Reliability* (France, Avignon, 2015)
9. A. Verma et al., Delineating the roles of Cr and Mo during ordering transformations in stoichiometric $Ni_2(Cr_{1-x}, Mo_x)$ alloys. Acta Mater. **96**, 366–377 (2015)
10. B. Gwalani et al., Experimental investigation of the ordering pathway in a Ni-33 at.%Cr alloy. Acta Mater. **115**, 372–384 (2016)
11. C. Pareige et al., Ordering and phase separation in Ni–Cr–Al: Monte Carlo simulations vs three-dimensional atom probe. Acta Mater. **47**(6), 1889–1899 (1999)